Evidence for Spin-Triplet Electron Pairing in the Proximity-Induced Superconducting State of an Fe-Doped InAs Semiconductor

Taketomo Nakamura, Le Duc Anh, Yoshiaki Hashimoto, Shinobu Ohya, Masaaki Tanaka, and Shingo Katsumoto

Phys. Rev. Lett. **122**, 107001 — Published 15 March 2019

DOI: 10.1103/PhysRevLett.122.107001

Evidence for spin-triplet electron pairing in the proximity-induced superconducting state of Fe-doped InAs semiconductor

Taketomo Nakamura[1],* Le Duc Anh[2,3], Yoshiaki Hashimoto[1],
Shinobu Ohya[2,3,4], Masaaki Tanaka[3,4], and Shingo Katsumoto[1,4]
[1]*Institute for Solid State Physics, University of Tokyo, 5-1-5 Kashiwanoha, Kashiwa, Chiba 277-8581, Japan*
[2]*Department of Electrical Engineering and Information Systems, University of Tokyo, 8-3-1 Hongo, Bunkyo, Tokyo 113-8656, Japan*
[3]*Institute of Engineering Innovation, Graduate School of Engineering, The University of Tokyo, 7-3-1 Hongo, Bunkyo-ku, Tokyo 113-8656, Japan and*
[4]*Center for Spintronics Research Network (CSRN), The University of Tokyo, 7-3-1 Hongo, Bunkyo-ku, Tokyo 113-8656, Japan*
(Dated: February 11, 2019)

We provide evidence for spin-triplet electron pairing in proximity-induced superconductivity in a ferromagnetic semiconductor (In, Fe)As. As discovered in half-metallic materials, extraordinary long proximity range is observed. More surprising is very strong concentration of supercurrent to the edges of the superconducting region, which is deduced from the extremely persistent oscillation of the critical current versus magnetic field. The maxima of the critical current appear not at the zero magnetic flux but at around the maximum magnetic disorder, reflecting the connectivity between the spin-triplet and singlet pairings. These spin-triplet natures in proximity superconductivity also reveal ferromagnetic properties of (In, Fe)As.

Coexistence of superconductivity and ferromagnetism has provided many subjects of interest in fundamental physics. A conventional Cooper pair of electrons with (momentum, spin) = $(\hbar\boldsymbol{k},\uparrow)$ and $(-\hbar\boldsymbol{k},\downarrow)$[1] requires modification of the (1) pair momenta or (2) spins to survive under a ferromagnetic exchange potential. In (1), such pairs have a non-zero total momentum, and are called Fulde-Ferrell-Larkin-Ovchinnikov (FFLO) states[2–5]. In (2), spin-triplet pairing (STP) takes place and results in a spin-polarized supercurrent; in other words, a super-spincurrent. The STP was introduced to explain the superfluidity of ^{3}He[6] and has attracted attention for its exotic properties. In bulk materials STP-based superconductivity has been claimed in uranium-based superconductors[7, 8] and Sr_2RuO_4[9, 10].

Heterogeneous junctions of ferromagnets and superconductors also offer potential emergence of STP through the proximity effect. In such systems, fascinating phenomena are predicted such as the appearance of Majorana fermions[11–13] or odd frequency superconductivity[14–20]. In experiments, observations of STP were claimed in superconducting junctions with a half-metal[21–23] and ferromagnetic multilayers[24, 25]. The most peculiar and strongest support for STP in these is extraordinary long range of the proximity effect.

Here, we ask whether the long range is the only unconventional property of STP-based superconductivity in junctions. To answer this experimentally, we chose (In, Fe)As (IFA) as the ferromagnet, inside which proximity superconductivity is induced by Nb electrodes. IFA is one of the III-V based ferromagnetic semiconductors (FMSs)[26–29]. As in many other III-V FMSs, half-metallic ferromagnetism is expected in IFA though not experimentally certified yet. In addition to that, the lack of spatial inversion symmetry and strong spin-orbit interaction (SOI) should lead to somewhat gradual connection between singlet and triplet superconductivities. The magnetic inhomogeneity is naturally introduced from the random distribution of magnetic ions. In particular, the magnetism is soft, which makes the response to the magnetic field continuous, highlighting the characteristics of superconductivity. N-type IFA[30] also offers electric contact to Nb with low resistances as a result of the natural downward band-bending at the surfaces of the indium-based semiconductors[31].

In this letter, we report the observation of proximity-induced supercurrents in IFA. The range of the proximity effect reaches about 1 μm at around 100 mK. The damping of oscillation in the critical current against the magnetic field is surprisingly slow, manifesting the confinement of the supercurrent to very narrow regions. Moreover, the peak of the critical current appears at magnetic fields far from the positions for zero magnetic flux, indicating the importance of demagnetizing fields for the proximity effect. These newly found unconventional behaviors constitute the evidence for STP in

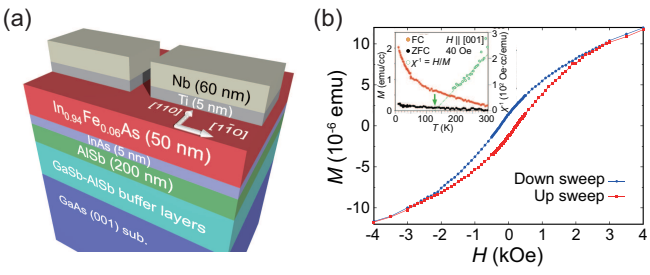

FIG. 1. (a) Schematic of the layered structure. (b) M (magnetization) -H (magnetic field) curve of the IFA film at 10 K measured with a dc-SQUID. The field direction is perpendicular to the film plane and the sweep range is $\pm$10 kOe. The inset shows the temperature dependence of the magnetization in IFA at H = 40 Oe for field cooling (FC, H = 10 kOe) and zero-field cooling (ZFC). The green open circles represent the inverse magnetic susceptibility indicating a Curie temperature of 128 K.

the proximity superconductivity.

A 50-nm-thick IFA film was grown by low-temperature molecular-beam epitaxy on a (001) GaAs substrate with GaSb/AlSb-based buffer layers, as illustrated in Fig.1(a). Details of the growth are given elsewhere[30]. The Fe concentration was 6% and the carrier concentration was estimated to be 8×10^{18} cm^{-3} at 3.5 K without doping of Be. The mean free path was estimated to be approximately 4 nm, shorter than the thickness of the IFA film. Figure 1(b) shows the magnetization curve of the present IFA film at 10 K, which exhibits clear hysteresis owing to ferromagnetism. The Curie temperature was estimated to be approximately 128 K from the temperature dependence of magnetic susceptibility, as shown in the inset of Fig.1(b). The devices are lateral-type junctions, in which the superconducting Nb electrodes with thin Ti adhesion layers were deposited on top of the IFA heterostructure, as illustrated in Fig.1(a). An optical micrograph image of the gap between the electrodes, which we henceforth call the "junction", is presented in Fig.2(a). The electric current direction was taken along [$\bar{1}$10] of the IFA crystal. This direction is optimal for generating a supercurrent in IFA, as examined previously[32]. In this experiment we prepared four junctions with gap lengths of 0.6, 0.8, 1.0, and 1.2 μm, which are named J06, J08, J10, and J12, respectively.

The Nb/Ti electrodes undergo the zero-resistance transition at around 6 K (T_c), which corresponds to a superconducting gap Δ_0 of 1.0 meV[33]. Figure 2(b) shows the temperature dependence of the zero-bias, zero-magnetic field resistance in J06. Below the T_c of Nb, the resistance remains constant down to 2 K, under which it starts decreasing again with decreasing temperature. The stepwise temperature variation indicates that the Nb/IFA interfacial resistance dominates the total resistance in the intermediate temperature region, and at around 2 K the superconducting proximity areas extending from the Nb electrodes begin to overlap. At the lowest temperature of about 0.1 K, all the junctions exhibit nonlinear I-V characteristics, namely, a dip structure in dV/dI around the zero-bias current, as shown in Fig.2(c). The zero-bias resistance of J08 is less than 20% of the normal resistance R_n, which cannot be explained by conductance enhancement due to Andreev reflection and small nonlinearity of IFA without the Josephson effect, and J06 exhibits clear zero resistance. To quantify the somewhat rounded rise of the resistance, we define the critical current I_c as the current at which the resistance recovers to $0.2R_n$. Figure 2(d) shows the distance dependence of the critical current and the zero-bias resistance. The critical current decreases with distance, indicating that the superconductivity is not bulk but the proximity effect. The proximity length is of an order similar to that in triplet proximity systems, as we discuss below[21, 24].

The magnetic field and bias current dependence of the dif-

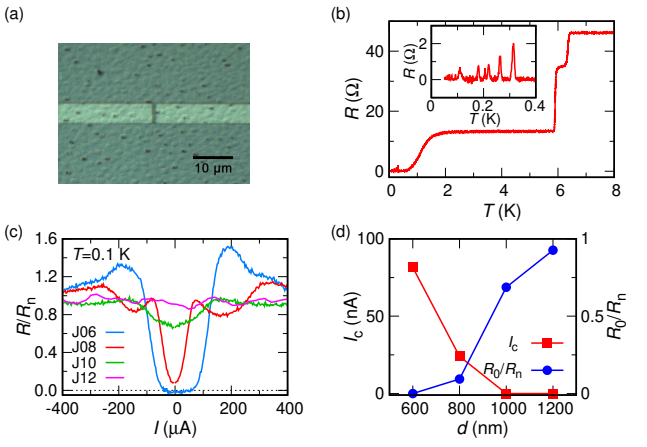

FIG. 2. (a) Optical micrograph image of the junction J10. (b) Temperature dependence of the zero-bias resistance of J06 at zero magnetic field. The inset shows close-up between 0 and 0.4 K. The resistance peaks are attibutable to domain wall motion discussed in the text. (c) Differential resistance as a function of the bias current for each junction in zero-field at 0.1 K. (d) Dependence of critical current and ratio of the zero-bias resistance R_0 to the normal resistance R_n on the gap length.

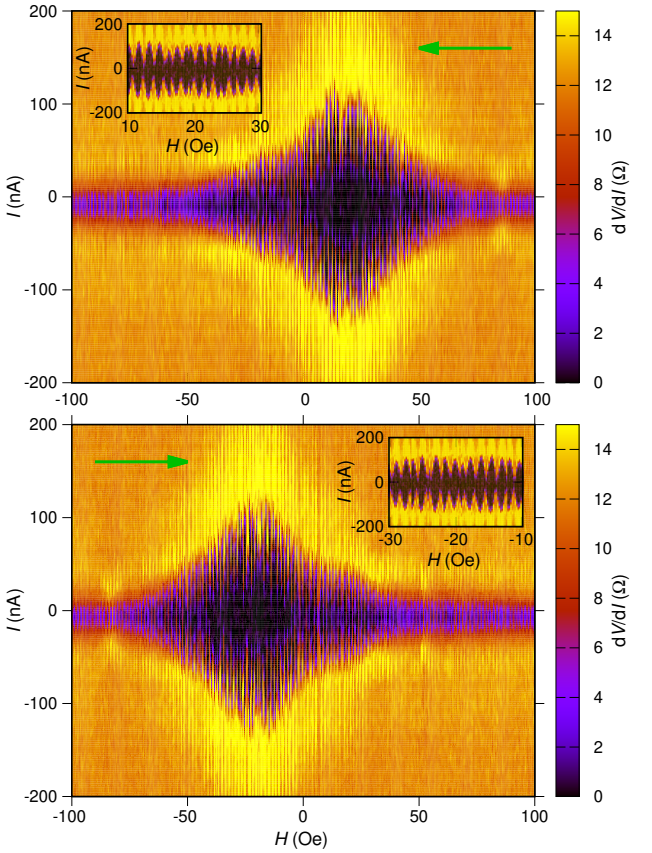

FIG. 3. Color plot of the differential resistance of J06 as a function of magnetic field and bias current. The field direction is perpendicular to the film plane. The external field was swept from $+109$ to -109 Oe for the upper panel, and the reverse for the lower panel, in which sweep directions are indicated by green arrows. The insets show close-ups around $+20$ and -20 Oe for down-sweep and up-sweep, respectively.

ferential resistance in J06 is shown in Fig.3. We observe fine regular oscillations in the differential resistance and the critical current against the perpendicular field. Each zero-resistance region in the oscillation is diamond-shaped on the H (magnetic field) -I (current) plane, as shown in the insets of Fig.3. This oscillatory field-dependence was also observed in J08, which evidences that the supercurrent originates from the Josephson effect. The observed period of 1.45 Oe is, however, shorter than the simple estimation of 5.17 Oe, corresponding to a single flux quantum $\Phi_0 = h/2e$ per junction area $A = (d + 2\lambda)w = 4$ μm^2, where the gap length $d = 600$ nm, electrode width $w = 5$ μm, and Nb penetration depth $\lambda = 100$ nm[34]. This short period is attributable to flux focusing caused by diamagnetism of the electrodes, that is, the magnetic field expelled from the electrodes are concentrated onto the junction area. The flux focusing can be taken into account by considering the effective junction area $A_{\rm eff}$, which is written as $f(t, d, w, \lambda)w^2$, where t is the thickness of Nb and a function $f(t, d, w, \lambda)$ is approximated by the constant 0.543 in the thin film region $t/\lambda < 2$[35]. With the present parameters, the effective junction area is calculated to be 13.6 μm^2, which corresponds to the period of 1.52 Oe in reasonable agreement with the experiment. Above 100 Oe, where the zero-bias resistance is finite, it still oscillates with the same period manifesting that the superconducting coherence remains in the junction. In J08 the resistance does not reach zero, though it also exhibits superconductivity through similar resistance oscillations against perpendicular fields.

Besides the period witdh the behavior in Fig.3 has more anomalous points as interference in a single Josephson junction. In an ordinary Fraunhofer pattern, $I_{\rm c}$ takes a maximum at the flux density $B_0 = 0$ G for a so-called 0-junction, or maxima at $B_\pi = \pm\Phi_0/(2A_{\rm eff}) = 0.76$ G for a π-junction, and decreases rapidly with magnetic field. The curve of $I_{\rm c}$ versus B is symmetric with respect to the origin $(B, I) = (0, 0)$ and independent of the field sweep direction. The anomalies can be summarized in the following two points: First, damping of the oscillation with the magnetic field is surprisingly weak, and the oscillation is observable up to 100 cycles. Second, $I_{\rm c}$ becomes maximum much earlier than the flux density $B = \mu_0 H + M$ (M: the magnetization) goes to zero, as explained below. $I_{\rm c}$s as a function of B for up and down sweeps are highly asymmetric with respect to the origin, and furthermore, they are hysteretic for the field sweeps. This indicates that the observed Josephson effect is caused by broken time-reversal symmetry, clearly reflecting the ferromagnetism in IFA. The envelope of the curve of $I_{\rm c}$ versus B for the up-sweep is mirror symmetric to that for the down-sweep about $H = 0$ when the sweep ranges are centered at $H = 0$ and after a few field sweeps in the same range. In combination with the magnetization curve for a wide field range in Fig.1(b), the above observations indicate that the M-H curve in these narrow-range sweeps also exhibits counter-clockwise loops around the origin of the M-H plane, probably due to the small coercive field and repeating field sweeps in the range. This means, for example, that M remains positive for the down-sweeps in the region of $H > 0$. In contrast, the envelope of $I_{\rm c}$ in the upper panel of Fig.3 reaches a peak around $+20$ Oe for the down-sweep, at which field the flux density $B = \mu_0 H + M$ should be finite and positive. In the same manner, we know that the peak for the up-sweep is around -20 Oe, at which B should be finite and negative.

Now, we look for a possible explanation of the above observations. Clear oscillations in the differential resistance versus magnetic field are observable in devices J06 and J08. That is, the superconducting coherence survives up to 0.8 μm in IFA[31, 36]. The conventional spin-singlet pairs, however, should be destroyed immediately away from the interface by the ferromagnetic exchange interaction[5, 37, 38]. The decay lengths of the spin-singlet and spin-triplet order parameters in ferromagnets are written as follows:

$$\begin{cases} \xi_{\rm d}^{\rm s} = \sqrt{\dfrac{\hbar D}{\sqrt{(\pi k_{\rm B}T)^2 + E_{\rm ex}^2} + \pi k_{\rm B}T}} & \text{(spin-singet)} \\ \xi_{\rm d}^{\rm t} = \sqrt{\dfrac{\hbar D}{2\pi k_{\rm B}T}} & \text{(spin-triplet),} \end{cases}$$

where D and $E_{\rm ex}$ are the diffusion coefficient and exchange energy in ferromagnets, respectively[39]. Anh *et al*. demonstrated that the exchange energies $E_{\rm ex}$ of IFA were well-explained by the Brillouin function[40]. According to them, we estimate $E_{\rm ex}$ of the present IFA to be 98 meV from the Curie's law and the Brillouin function. By using $D = 1.4 \times 10^{-3}$ m^2/s obtained from the measured mobility $\mu = 100$ cm^2/Vs of the present IFA film at 3.5 K, the decay length $\xi_{\rm d}^{\rm s}$ is estimated to be 3.1 nm at 0.1 K. The gap lengths of our devices are much longer than the distance where the spin-singlet order parameters from the Nb electrodes are expected to overlap with each other, even if we consider an empirical rule that we can observe the Josephson effect in junctions with gap lengths approximately ten times greater than $\xi_{\rm d}^{\rm s}$. On the other hand, $\xi_{\rm d}^{\rm t}$ is estimated to be 130 nm, reasonable length for our results. Therefore, the present pairing in the proximity-induced superconductivity must be spin-triplet. Note that $I_{\rm c}$ in this system is difficult to be estimated by theories since various factors contribute to generation of spin-triplet order parameters. Compared to Refs.[21, 24], the $I_{\rm c}R_{\rm n}$ value of about 1.7 μV at 0.1 K is smaller because of longer gap lengths, more diffusive ferromagnet, and mechanisms of singlet-triplet conversion.

Next, we consider the interference patterns in Fig.3. As the first point, the weak damping in amplitude and the regularity in the period of the oscillations indicate that the supercurrent is strongly localized at the two edges of the junction area, as calculated, *e.g.*, in Refs.[41, 42]. This cannot be explained by current localization within the Josephson penetration depth $\lambda_{\rm J} = (\hbar/2e\mu_0 d I_{\rm c})^{1/2}$, which is estimated to be about 15 μm in the present case, and still larger than the junction width w. Instead, the current localization is explained by the efficiency of singlet-triplet conversion via magnetic inhomogeneity[19]. Such inhomogeneity can be formed at the surface of III-V FMSs, *e.g.* by strain-induced magnetization-

reorientation[26]. Some strain exists at the interface between Nb/Ti and IFA owing to the difference of thermal expansion, and the strain must be concentrated to the corners of Nb electrodes. Hence the conversion efficiency should be higher around the corners, leading to the supercurrent localization. The significance of strain is not just imaginary but evidenced by the fact that the anisotropic surface strain strongly affects the Josephson effect; the I_c in [110] direction is one order smaller than that in [$\bar{1}$10] direction[32], which cannot be explained by neither the anisotropy in the magnetism of IFA[43] nor that in the transport.

The second point—the peak positions of the envelope—provides important information. Inside the film, the flux density is still $\mu_0 H + M$, while the magnetic field is $H_{\rm in} = H + NM/\mu_0$, where N, the demagnetization coefficient, is nearly -1 for thin films. Assuming an M-H curve similar to that in Fig.1(b) for the minor loop in Fig.3, and considering the flux-concentration effect, we identify the peak positions corresponding to $H_{\rm in} \sim 0$. In superconductivity with singlet pairing, there is no such electromagnetic freedom that picks up the local magnetic field, though the spin of Cooper pairs can perform this in the triplet pairing superconductivity. More specifically, because of the granularity in the ferromagnetism of IFA, the randomness of the magnetization inside the film should become maximum at $H_{\rm in} = 0$, and this could be the best condition for the triplet proximity effect from singlet superconductors[44].

The granularity of the ferromagnetism also appears in the minor loop behavior. In Fig.4, we plot the field dependence of the zero-bias differential resistance (ZBR) in different sweep ranges. The ZBR curves are hysteretic when the sweep range exceeds 90 Oe, as shown in Fig.4(a)(b), but no hysteresis is observable for a sweep range narrower than 30 Oe, as shown in Fig.4(c). This behavior reflects the granular ferromagnetism in IFA and some ratchet-like mechanisms, which prevent the instantaneous reversal of domain wall motion and are initiated between 30 and 90 Oe.

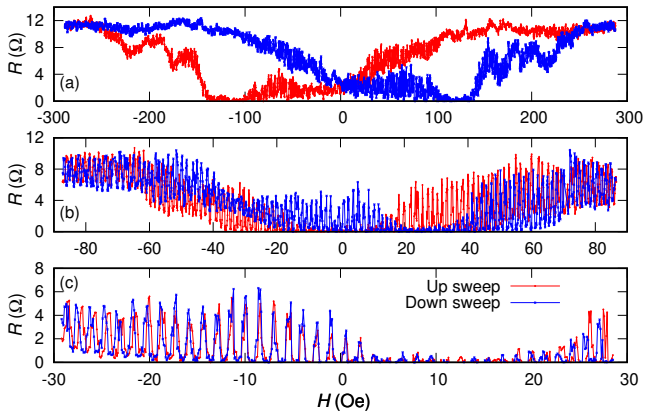

FIG. 4. Field dependence of the zero-bias differential resistance of J06. The field was swept sequentially via the following points: +14 kOe, −290, 290, −290, 290, −90, 90, −90, 90, −30, 30, −30, and 30 Oe. The panels are the data for the sweeps from (a) −290 to −290 Oe via +290 Oe, (b) −90 to −90 Oe via +90 Oe, and (c) −30 to −30 Oe via +30 Oe.

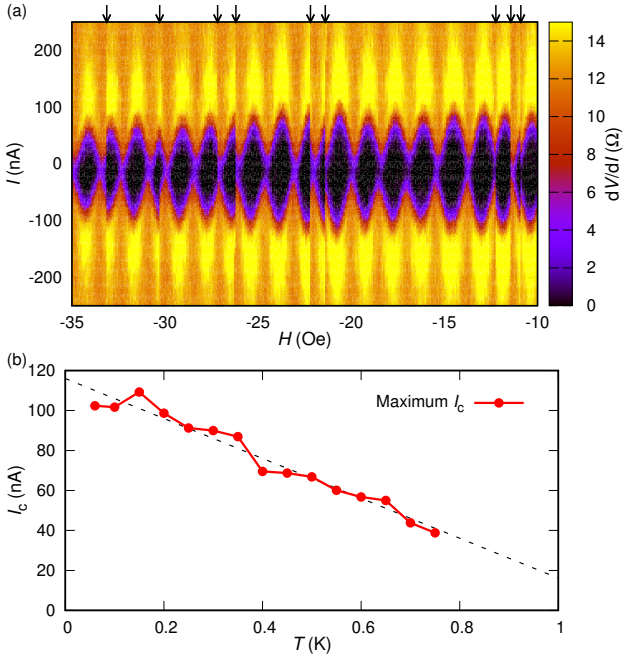

FIG. 5. (a) Color plot of the differential resistance of J06 as a function of the magnetic field and bias current at 0.35 K. After the field was swept to −109 Oe, the resistance was measured from −36 to −8 Oe. The arrows above the graph indicate the phase slip attributable to the domain wall motion. (b) Temperature dependence of the maximum critical current of J06 in the range between −36 and −8 Oe. The broken line is a fitting line of the data.

Such domain motion sometimes contains jumps in the fluxoid at the junction, which are observable in the oscillation pattern in Fig.5(a). These jumps cause a discontinuity in the phase of the I_c oscillation but keep the envelope continuous, which is consistent with our interpretation that the interference pattern depends on the magnetic flux piercing the junction area while the current is localized at the edges, and the amplitude is determined by the condition of singlet-triplet connection. The emergence of finite resistance below 0.5 K shown in Fig.2(b) is also caused by this discontinuous phase slip, indicating domain wall motion by the temperature sweep. This makes it difficult to fix the phase difference during the measurement of the temperature dependence of I_c. To avoid this difficulty, we performed the same measurement as in Fig.5(a) and obtained the maximum I_c in the range between −36 and −8 Oe for the up-sweep at various temperatures. Figure 5(b) illustrates the temperature dependence of the maximum I_c thus obtained, which monotonically decreases with temperature in the same manner as in previous studies[21].

Thus far we have seen that the STP scenario can explain all the observations, whereas the conventional spin-singlet picture cannot evade essential difficulties. At the same time, IFA is expected to satisfy several conditions to induce STP from

singlet superconductors, *e.g.*, inhomogeneous magnetization, SOI, and high spin polarization. As we discussed above, the inhomogeneous magnetization appears as strain-induced magnetization reorientation and magnetic domains. In addition, strong SOI exists in IFA as a narrow-gap semiconductor. Although the SOI inevitably leads to some mixing of singlet-triplet superconductivity, only the triplet component survives in IFA bacause of its ferromagnetic exchange interaction[40]. Note that the present IFA film has a fairly short mean free path and is close to the dirty limit. From the study of the impurity effect in noncentrosymmetric superconductors, it has been clarified that, even when the SOI is finite, the s-wave coupling can be dominant. We then conclude that the s-wave STP, which was observed in the S/HM/S junctions[21], is dominant in the observed superconducting proximity effect. The present work opens the possibility to investigate the exotic natures of spin-triplet superconductivity in a wide range of parameters or material combinations by using tunability in the ferromagnetism of IFA through, *e.g.*, the content of Fe, carrier concentration or application of gate voltage.

We wish to thank Y. Asano for his fruitful discussions. This work was supported by Grants-in-Aid for Scientific Research on Innovative Areas, "Nano Spin Conversion Science" (Grant No. JP26103003) and "Topological Materials Science" (Grant No. JP18H04218), JSPS KAKENHI Grant Numbers JP25247051, JP17K05492, JP17H04922, and JP18H03860, CREST Program of JST (No. JPMJCR1777), Spintronics Research Network of Japan, and Special Coordination Funds for Promoting Science and Technology.

* taketomo@issp.u-tokyo.ac.jp

[1] M. Tinkham, *Introduction to Superconductivity: Second Edition* (Dover Publications, INC., 2004).
[2] P. Fulde and R. A. Ferrell, Phys. Rev. **135**, A550 (1964).
[3] A. I. Larkin and Y. N. Ovchinnikov, Zh. Eksp. Teor. Fiz. **47**, 1136 (1964).
[4] Y. Matsuda and H. Shimahara, Journal of the Physical Society of Japan **76**, 051005 (2007), https://doi.org/10.1143/JPSJ.76.051005.
[5] T. Kontos, M. Aprili, J. Lesueur, F. Genêt, B. Stephanidis, and R. Boursier, Phys. Rev. Lett. **89**, 137007 (2002).
[6] A. J. Leggett, Rev. Mod. Phys. **47**, 331 (1975).
[7] R. Joynt and L. Taillefer, Rev. Mod. Phys. **74**, 235 (2002).
[8] V. P. Mineev, Physics-Uspekhi **60**, 121 (2017).
[9] A. P. Mackenzie and Y. Maeno, Rev. Mod. Phys. **75**, 657 (2003).
[10] Y. Maeno, S. Kittaka, T. Nomura, S. Yonezawa, and K. Ishida, Journal of the Physical Society of Japan **81**, 011009 (2012), https://doi.org/10.1143/JPSJ.81.011009.
[11] M. Sato and S. Fujimoto, Journal of the Physical Society of Japan **85**, 072001 (2016), https://doi.org/10.7566/JPSJ.85.072001.
[12] R. M. Lutchyn, J. D. Sau, and S. Das Sarma, Phys. Rev. Lett. **105**, 077001 (2010).
[13] Y. Oreg, G. Refael, and F. von Oppen, Phys. Rev. Lett. **105**, 177002 (2010).
[14] A. F. Volkov, F. S. Bergeret, and K. B. Efetov, Phys. Rev. Lett. **90**, 117006 (2003).
[15] Y. Asano, Y. Sawa, Y. Tanaka, and A. A. Golubov, Phys. Rev. B **76**, 224525 (2007).
[16] Y. Tanaka, M. Sato, and N. Nagaosa, Journal of the Physical Society of Japan **81**, 011013 (2012), https://doi.org/10.1143/JPSJ.81.011013.
[17] F. S. Bergeret, A. F. Volkov, and K. B. Efetov, Rev. Mod. Phys. **77**, 1321 (2005).
[18] A. I. Buzdin, Rev. Mod. Phys. **77**, 935 (2005).
[19] M. Eschrig and T. Löfwander, Nat. Phys. **4**, 138 (2008).
[20] J. Linder and J. W. A. Robinson, Nat. Phys. **11**, 307 (2015).
[21] R. Keizer, S. Goennenwein, T. Klapwijk, G. Miao, G. Xiao, and A. Gupta, Nature **439**, 825 (2006).
[22] M. S. Anwar, F. Czeschka, M. Hesselberth, M. Porcu, and J. Aarts, Phys. Rev. B **82**, 100501 (2010).
[23] D. Sprungmann, K. Westerholt, H. Zabel, M. Weides, and H. Kohlstedt, Phys. Rev. B **82**, 060505 (2010).
[24] J. W. A. Robinson, J. D. S. Witt, and M. G. Blamire, Science **329**, 59 (2010), http://science.sciencemag.org/content/329/5987/59.full.pdf.
[25] T. S. Khaire, M. A. Khasawneh, W. P. Pratt, and N. O. Birge, Phys. Rev. Lett. **104**, 137002 (2010).
[26] T. Dietl and H. Ohno, Rev. Mod. Phys. **86**, 187 (2014).
[27] H. Munekata, H. Ohno, S. von Molnar, A. Segmüller, L. L. Chang, and L. Esaki, Phys. Rev. Lett. **63**, 1849 (1989).
[28] H. Ohno, A. Shen, F. Matsukura, A. Oiwa, A. Endo, S. Katsumoto, and Y. Iye, Appl. Phys. Lett. **69**, 363 (1996).
[29] T. Hayashi, M. Tanaka, T. Nishinaga, H. Shimada, H. Tsuchiya, and Y. Otuka, J. Cryst. Growth **175**, 1063 (1997).
[30] P. Nam Hai, L. Duc Anh, S. Mohan, T. Tamegai, M. Kodzuka, T. Ohkubo, K. Hono, and M. Tanaka, Appl. Phys. Lett. **101**, 182403 (2012), http://dx.doi.org/10.1063/1.4764947.
[31] T. Schäpers, *Superconductor/Semiconductor Junctions* (Springer, 2011).
[32] T. Nakamura, L. D. Anh, Y. Hashimoto, Y. Iwasaki, S. Ohya, M. Tanaka, and S. Katsumoto, Journal of Physics: Conference Series **969**, 012036 (2018).
[33] A. V. Pronin, M. Dressel, A. Pimenov, A. Loidl, I. V. Roshchin, and L. H. Greene, Phys. Rev. B **57**, 14416 (1998).
[34] A. I. Gubin, K. S. Il'in, S. A. Vitusevich, M. Siegel, and N. Klein, Phys. Rev. B **72**, 064503 (2005).
[35] P. A. Rosenthal, M. R. Beasley, K. Char, M. S. Colclough, and G. Zaharchuk, Applied Physics Letters **59**, 3482 (1991).
[36] H. Irie, Y. Harada, H. Sugiyama, and T. Akazaki, Phys. Rev. B **89**, 165415 (2014).
[37] M. Weides, M. Kemmler, E. Goldobin, D. Koelle, R. Kleiner, H. Kohlstedt, and A. Buzdin, Applied Physics Letters **89**, 122511 (2006), https://doi.org/10.1063/1.2356104.
[38] F. Born, M. Siegel, E. K. Hollmann, H. Braak, A. A. Golubov, D. Y. Gusakova, and M. Y. Kupriyanov, Phys. Rev. B **74**, 140501 (2006).
[39] A. I. Buzdin, B. Bujicic, and M. Y. Kupriyanov, Sov. Phys. JETP **74**, 124 (1992).
[40] L. D. Anh, P. N. Hai, and M. Tanaka, Nature Communications **7**, 13810 (2016).
[41] A. Barone, G. Paternò, M. Russo, and R. Vaglio, physica status solidi (a) **41**, 393 (1977).
[42] A. Barone and G. Paterno, *Physics and Applications of the Josephson Effect*, 1st ed. (Wiley-VCH, 1982).
[43] P. Nam Hai, D. Sasaki, L. D. Anh, and M. Tanaka, Applied Physics Letters **100**, 262409 (2012), https://doi.org/10.1063/1.4730955.
[44] S. Hikino and S. Yunoki, Phys. Rev. Lett. **110**, 237003 (2013).